Title

Examining air pollution exposure dynamics in disadvantaged communities through high-resolution mapping.

Journal

Science Advances, 10(32)

Authors

Su, Jason
Aslebagh, Shadi
Vuong, Vy
et al.

Publication Date

2024-08-09

DOI

10.1126/sciadv.adm9986

Peer reviewed

PUBLIC HEALTH

Examining air pollution exposure dynamics in disadvantaged communities through high-resolution mapping

Jason G. Su[1]*, Shadi Aslebagh[1], Vy Vuong[2], Eahsan Shahriary[1], Emma Yakutis[1], Emma Sage[1], Rebecca Haile[1], John Balmes[3], Michael Jerrett[4], Meredith Barrett[2,5]

This study bridges gaps in air pollution research by examining exposure dynamics in disadvantaged communities. Using cutting-edge machine learning and massive data processing, we produced high-resolution (100 meters) daily air pollution maps for nitrogen dioxide (NO_2), fine particulate matter ($PM_{2.5}$), and ozone (O_3) across California for 2012–2019. Our findings revealed opposite spatial patterns of NO_2 and $PM_{2.5}$ to that of O_3. We also identified consistent, higher pollutant exposure for disadvantaged communities from 2012 to 2019, although the most disadvantaged communities saw the largest NO_2 and $PM_{2.5}$ reductions and the advantaged neighborhoods experienced greatest rising O_3 concentrations. Further, day-to-day exposure variations decreased for NO_2 and O_3. The disparity in NO_2 exposure decreased, while it persisted for O_3. In addition, $PM_{2.5}$ showed increased day-to-day variations across all communities due to the increase in wildfire frequency and intensity, particularly affecting advantaged suburban and rural communities.

INTRODUCTION

Environmental justice research has shed light on the disproportionate air pollution burdens carried by disadvantaged communities, yet a critical gap persists. Prior investigations, for the most part, have operated within broad timeframes, often focusing on annual assessments (*1*). These examinations typically relied on summarizations lacking small-area variations (e.g., >5 km) and drew from the limited data provided by widely spaced regulatory monitoring stations (*2*). Consequently, the fine-grained, day-to-day fluctuations in pollutant concentrations affecting disadvantaged communities have remained largely undetected. Disadvantaged communities are often situated near manufacturing and industrial facilities that emit a substantial amount of pollutants into the air (*3*–*5*). Disadvantaged communities may also be adjacent to major roadways and transportation routes that contribute to elevated levels of vehicular emissions (*6*–*8*). These systemic issues contribute to higher levels of air pollution exposure, which can lead to adverse health outcomes for the residents of these communities (*9*–*11*). However, many studies, especially those modeling daily exposures through remote sensing data (e.g., high-resolution aerosol optical depth data of 1-km resolution) or dispersion modeling techniques (typically in the range of 1 to 10 km), cannot distinguish their specific exposure from those living in less polluted areas due to limitations in spatial resolution and data availability (*12*).

Land use, land cover, meteorological conditions, elevation, and other factors influence air pollution concentrations. Previous exposure assessments have primarily relied upon air pollutant concentrations measured from the nearest regulatory monitoring sites, which are sparsely distributed and reflect the background concentrations of a region. Using the nearest regulatory site as proxy for exposure assumes the monitoring site and community share the same land use and land cover. Regulatory monitoring data sometimes are used as inputs for air pollution exposure assessments through techniques such as kriging or inverse distance weighting (*13*). Those techniques used regulatory sites for exposure assessment; however, they still assumed the same land use and land cover information of the community as those of regulatory sites. Relying solely on regulatory monitoring data for exposure proxy may complicate the exploration of exposure disparities, as the resolution of the data may be insufficient to adequately inform such disparities, particularly regarding differences in exposure and land use between disadvantaged and advantaged communities.

Integrating land use regression (LUR) modeling into exposure assessments presents a promising avenue for addressing this challenge. LUR modeling applies land use, land cover, and other related information to model pollutant concentrations measured at monitoring sites (*14*, *15*). LUR modeling advances exposure assessment by using factors that affect a community's pollutant concentrations. LUR is typically used to model pollutant concentrations at the city or metropolitan level, and it can achieve high spatial resolution, such as 30 m, which is especially true for annual LUR models and surfaces. Traditional LUR models, however, suffer from overfitting when the data are used for model construction and performance assessment (*16*).

Daily air pollution models are important for identifying health effects due to short-term air pollution exposures and are largely developed through machine learning algorithms. For example, the random forest modeling technique has been increasingly used to model daily air pollutant concentrations with remote sensing data (*17*–*21*). These algorithms can deal with model overfit, multicollinearity among predictors, and potential nonlinear associations between a predictor and air pollutant concentrations. However, they cannot remove potential redundant or statistically nonsignificant predictors in the modeling process. With hundreds and sometimes thousands of potential predictors, a machine learning algorithm might generate results that are hard to interpret. In addition, they are less adept at modeling high spatial resolution. Last, most annual and daily LUR models use only one type of monitoring data: 1)

[1]School of Public Health, University of California, Berkeley, Berkeley, CA 94720, USA. [2]Propeller Health, 505 Montgomery St. #2300, San Francisco, CA 94111, USA. [3]School of Medicine, University of California, San Francisco, San Francisco, CA 94143, USA. [4]Fielding School of Public Health, University of California, Los Angeles, Los Angeles, CA 90095, USA. [5]ResMed, San Diego, CA 92123, USA.
*Corresponding author. Email: jasonsu@berkeley.edu

regulatory monitoring, 2) fixed site saturation monitoring, or 3) mobile low-cost sensor monitoring. Integrating all three sources into a single modeling framework has yet to be seen in the literature.

We aimed to address these previous limitations by generating a comprehensive dataset for modeling air pollution exposure, incorporating terabytes of data from all three monitoring sources, including Google Streetcar data, to develop models that would predict daily surfaces at a high spatiotemporal resolution, accounting for hundreds of unique community-level covariates. We focused on three criteria air pollutants for which National Ambient Air Quality Standards are established—nitrogen dioxide (NO_2), fine particulate matter with aerodynamic diameter ≤2.5 μm ($PM_{2.5}$), and ozone (O_3)—all of which have demonstrated impacts on health (*22*–*28*). We targeted the state of California, the nation's most populous state and one-seventh of the U.S. economy and evaluated trends over time (2012 to 2019). The high spatiotemporal air pollution surfaces allowed us to identify disparities by neighborhood disadvantage status, race-ethnicity, geographic location, and over time across California.

Overall, this study pioneers a previously unidentified approach by developing high spatiotemporal resolution daily air pollution surfaces (100 m), enabling a granular examination of the nuanced exposure disparities for disadvantaged communities, even as overall air pollution concentrations decrease. Our research aims to identify and understand environmental injustices, particularly how air pollution exposure trends differ between disadvantaged and advantaged communities. We hypothesize that targeted policy interventions focused on mitigating industrial and transportation-related emissions and enhancing air quality have predominantly benefited residents in marginalized neighborhoods. Despite observed overall air quality improvements, we aim to determine whether disparities persist, with disadvantaged communities continuing to experience higher exposure levels. This study will provide critical insights and methodological advancements necessary to identify air pollution exposure disparities, guiding future policy decisions as data availability increases.

RESULTS

Pollutant model development

For the NO_2 model, the total number of predictors and associated buffered distance statistics (covariates) was 2157, which was reduced to 140 via data reduction. The model had an adjusted R^2 of 79.6% (table S1). We highlight four predictors based on their significance and strong association with air pollution concentrations, as determined through correlation analysis. They included vehicle kilometers traveled (VKT), percentage of impervious surface, hectare of high-intensity developed land cover, and hectare of forest trees. Specifically, these predictors have demonstrated correlation coefficients greater than 0.15, indicating a substantial relationship with measured pollutant concentrations. Moreover, these predictors align with the variables traditionally used in LUR modeling, which aims to capture spatial variations in air pollution concentrations based on land use, land cover, and other relevant factors. By showcasing these predictors, we aim to illustrate their distance decay correlation with measured concentrations, providing insight into their influence on local air quality patterns. The buffer distance statistics in Fig. 1 for a predictor ranged from 50 to 5 km at an interval of 50 m, except for VKT that ranged from 50 to 2 km. The curves

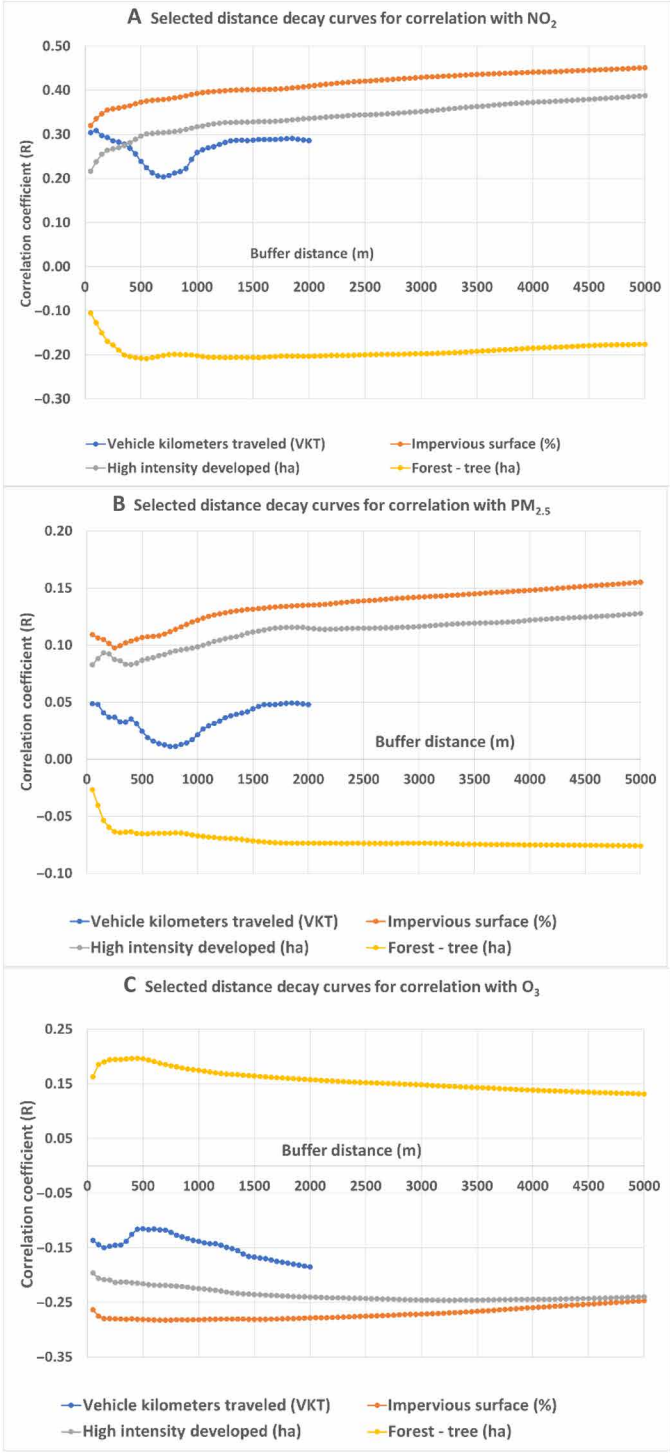

Fig. 1. The distance decay curves of correlation with air pollutants for selected predictors. The three pollutants include (**A**) nitrogen dioxide (NO_2), (**B**) fine particulate matter ($PM_{2.5}$), and (**C**) ozone (O_3). The buffer distance statistics for a predictor ranged from 50 m to 5 km at an interval of 50 m, except for VKT that ranged from 50 m to 2 km. The curves represent how the strength of correlation between each predictor and the respective air pollutant changes with increasing distance from the pollution source. This analysis provides insights into the spatial relationships and influences of various predictors on air quality across different distances.

represent how the strength of correlation between each predictor and the respective air pollutant changes with increasing distance from the pollution source. This analysis provides insights into the spatial relationships and influences of various predictors on air quality across different distances. VKT had the highest impact on NO_2 concentrations, peaking at 100 m within a roadway and declining to the lowest at 700 m before rising again at the 2000-m buffer (Fig. 1A). Percent impervious surface and high-intensity developed land were also positively associated with NO_2, with a rapid increase within the first 200 m and then gradually increasing to the 5000-m buffer. By contrast, forests/trees, shrublands, water, wetlands, developed open space, and residential land use were all negatively associated with NO_2 concentrations (as a sink or lack of emissions). Temporally, winter months were associated with higher concentrations and weekend days with lower concentrations. Figure S2 displays daily (01 January), monthly (January), and annual NO_2 surfaces for 2012 across California.

For the $PM_{2.5}$ model, the total number of predictors and associated buffered distance statistics was 2159, reduced to 145 via data reduction. The model had an adjusted R^2 of 65.3% (table S2). Predictors in the model had similar directions of association as seen in the NO_2 model, including VKT, percent impervious surface, intensely developed land cover, and forests/trees (negative), but the strength of the relationship between our predictors and observed $PM_{2.5}$ concentrations, represented by correlation coefficients, were much smaller (Fig. 1B). Figure S3 displays daily (01 January), monthly (January), and annual $PM_{2.5}$ surfaces for 2012 across California.

For the O_3 model, the total number of predictors and associated buffer statistics was 2157, reduced to 126 via data reduction. The final O_3 model had a prediction power of 93.6% (adjusted R^2), with its predictors largely showing opposite directions of association compared to those for NO_2 and $PM_{2.5}$ (table S3 and Fig. 1C). Figure S4 displays daily (01 January), monthly (January), and annual O_3 surfaces for 2012 across California.

Air pollution exposure disparities

Disparities in air pollution exposure by disadvantage status

We examined mean annual air pollution concentrations across California's disadvantaged and advantaged census tracts (referred to as communities hereafter), as defined by the CalEnviroScreen (*29*) cumulative score (≥75th percentile for disadvantaged versus ≤25th percentile for advantaged). In 2012, disadvantaged communities demonstrated substantially higher mean annual concentrations for all three pollutants versus the least disadvantaged communities, respectively: 12.50 versus 7.36 parts per billion (ppb) for NO_2, 11.92 versus 8.47 μg/m3 for $PM_{2.5}$, and 34.45 versus 34.01 ppb for O_3 (all $P < 0.05$). This trend was maintained through 2019, with 10.39 versus 6.06 ppb for NO_2, 10.75 versus 7.49 μg/m3 for $PM_{2.5}$, and 34.84 versus 34.74 ppb for O_3 for most disadvantaged versus least disadvantaged. The differences were statistically significant for all years ($P < 0.05$), except for O_3 in 2019 ($P = 0.31$).

Disparities in air pollution exposure by geographic location

We mapped air pollution exposure disparities for California's four major metropolitan areas: San Francisco Bay Area (SF Bay), Los Angeles Metropolitan area (LA Metro), Sacramento, and Fresno (Fig. 2), and examined the communities in which the highest air pollution exposure occurred (defined as ≥75th percentile for each pollutant at annual concentration). For NO_2 (left column), the LA Metro had the highest concentrations in the state, with 78.7% of disadvantaged communities and 17.1% of advantaged communities experiencing high concentrations (i.e., more than 75th percentile of NO_2 concentrations). The highest concentrations in LA were seen in central traffic corridors, coincident with most disadvantaged communities. In the SF Bay, the West Oakland community showed the highest concentrations. Overall, 6.2% of disadvantaged communities in SF Bay had high concentrations, while no advantaged communities demonstrated such concentrations (table S4). Both Sacramento and Fresno showed relatively lower concentrations of NO_2 concentrations; however, disparities in exposure by disadvantage still existed (e.g., 4.0 and 0.1% disadvantaged communities, respectively, in Sacramento and Fresno, for high concentrations but with 0.0% for their advantaged communities). Statewide, higher proportions of disadvantaged communities had higher NO_2 concentrations in all metropolitan areas.

For $PM_{2.5}$, the LA Metro had the highest concentrations in the State, with 70.4% of disadvantaged communities and 5.0% of advantaged communities having high concentrations (table S4). The highest

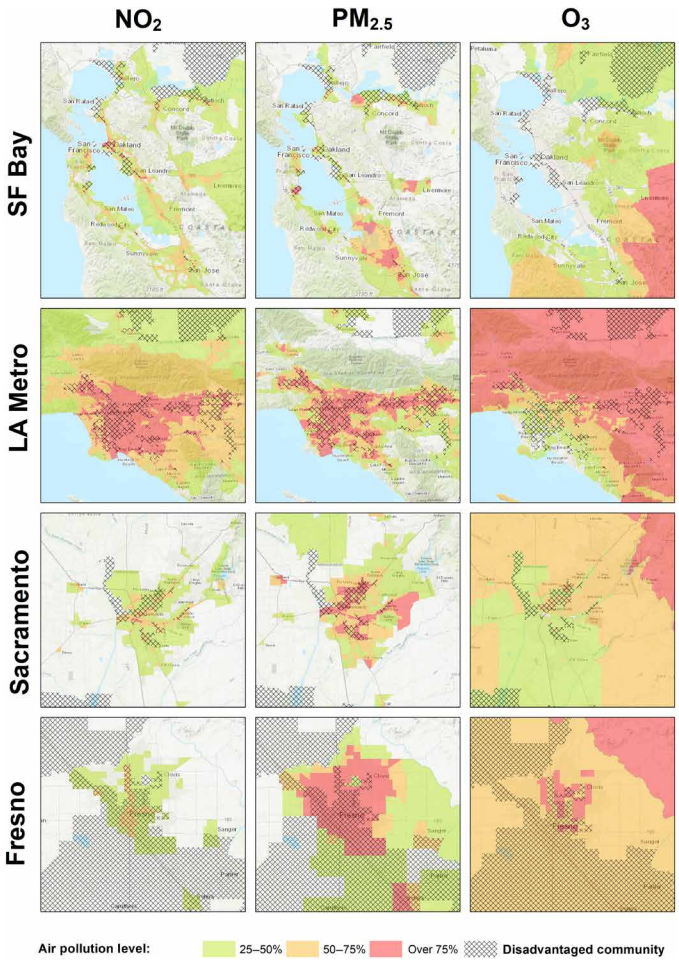

Fig. 2. Annual mean concentrations of nitrogen dioxide (NO_2), fine particulate matter ($PM_{2.5}$), and ozone (O_3), categorized by percentile (with that more than 75% as high pollutant concentrations), for four major metropolitan areas in California: San Francisco Bay Area, Los Angeles metropolitan area, Sacramento, and Fresno metros. The crosshatching indicates areas of the most disadvantaged communities.

concentrations were found along traffic corridors where the most disadvantaged communities reside (Fig. 2, middle). Fresno also experienced high concentrations, with 67.3% of disadvantaged communities and 61.9% of advantaged communities having high concentrations. Central Fresno experienced the highest concentrations. For Sacramento, 62.0% of disadvantaged communities had high concentrations, and the central part of Sacramento overlapped with the disadvantaged communities. In the SF Bay, 6.2% of disadvantaged communities and 1.3% of advantaged communities experienced high concentrations, with the most disadvantaged communities mainly distributed in the northern part of the region. Like NO_2, higher proportions of disadvantaged communities had high $PM_{2.5}$ concentrations in all metropolitan areas.

For O_3 (Fig. 2, right), spatial distributions showed opposite patterns of NO_2 and $PM_{2.5}$, with generally higher concentrations found at the outskirts of the four metropolitan areas. For LA Metro, 16.0% of disadvantaged and 25.1% of advantaged communities had high concentrations (fig. S4). These numbers were similar to Fresno, with 16.4 and 23.8% of disadvantaged and advantaged communities experiencing high concentrations, respectively. For both LA Metro and Fresno, higher proportions of advantaged communities had higher concentrations than disadvantaged communities. By comparison, the SF Bay and Sacramento areas had relatively low concentrations, and their concentrations were still lower in urban cores compared to surrounding regions (Fig. 2).

Disparities in air pollution exposure by race-ethnicity

The median CalEnviroScreen scores for the most and least disadvantaged communities were 49.7 and 9.8, respectively. The corresponding race-ethnicity compositions of white and Hispanic were 9.6 and 68.6% for the most disadvantaged tracts and 66.8 and 12.4% for the least disadvantaged tracts, respectively. African Americans and Asian Americans had relatively low percentages in population composition across the state but still showed higher percentages of African Americans and lower percentages of Asian Americans in the most disadvantaged group (4.2 and 4.9%) compared to the most advantaged group (1.3 and 9.2%).

Figure 3 shows race-ethnicity associations with air pollution exposure at a community level, separately for O_3, $PM_{2.5}$, and NO_2, in three multivariable models. For the NO_2 model, results largely showed that communities with a higher composition of Hispanic, African American, and Asian Americans were associated with higher NO_2 versus communities with higher white composition. $PM_{2.5}$ demonstrated similar trends, with less-white communities experiencing higher exposure to $PM_{2.5}$, but the estimated differences between white and non-white were not as large as with NO_2.

Conversely, these relationships were reversed for O_3: Communities with higher white compositions were associated with higher concentrations of O_3. Associations were slightly lower for communities with higher Hispanic compositions but much lower for communities with higher African American and Asian American composition.

Air pollution exposure disparity trends

For NO_2 and $PM_{2.5}$, concentrations decreased from 2012 to 2019 for all communities in California. On average, NO_2 decreased by 2.11 (16.9%) and 1.30 ppb (17.7%), for disadvantaged and advantaged communities. $PM_{2.5}$ decreased by 1.17 (9.8%) and 0.98 μg m^{-3} (11.6%), for disadvantaged and advantaged communities, respectively. By contrast, for disadvantaged and advantaged communities, O_3 increased by 0.39 (1.1%) and 0.73 ppb (2.1%). We modeled

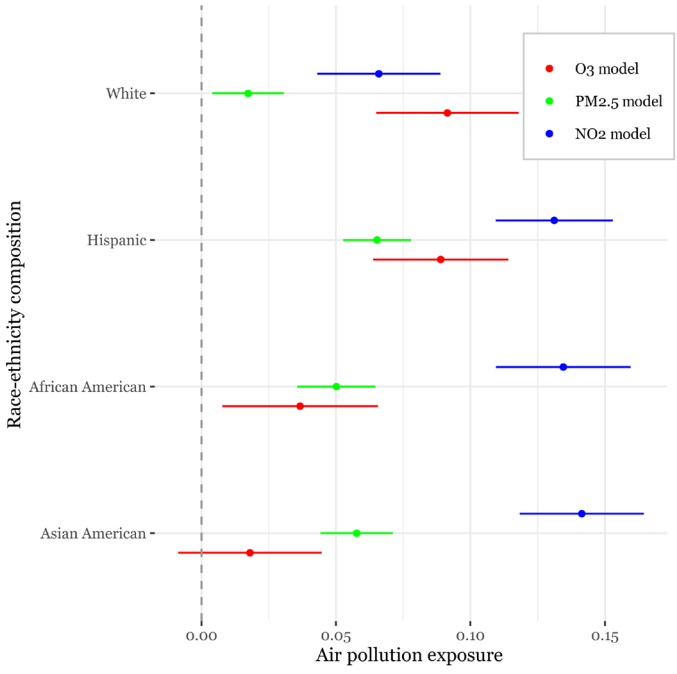

Fig. 3. The multivariate associations of race-ethnicity composition, defined by the percentage of each community population, with air pollution concentrations, respectively, for nitrogen dioxide, NO_2 (blue), fine particulate matter, $PM_{2.5}$ (green), and ozone, O_3 (red).

interactions between year and cumulative census tract disadvantage categories [disadvantaged (75th to 100th percentile), medium (26th to 74th percentile), and advantaged (1st to 25th percentile score)], identifying their associations with air pollution exposure at a community level. Figure 4 displays trends of mean annual air pollution concentrations for NO_2, $PM_{2.5}$, and O_3 for the most, medium, and least disadvantaged communities. The most disadvantaged communities saw a steeper decline in NO_2 and $PM_{2.5}$ concentrations during this period compared with the least disadvantaged communities (−0.29 versus −0.21 slope for NO_2, −0.12 versus −0.1 for $PM_{2.5}$). Conversely, we found that O_3 increased for all levels of disadvantage from 2012 to 2019, but advantaged communities had the greatest increase (+0.11 versus 0.09 slope). For all three pollutants, we found that disparities in air pollution exposure decreased from 2012 to 2019 (Fig. 4).

Air pollution exposure day-to-day fluctuations

Figure 5 displays trends of day-to-day fluctuations from 2012 to 2019 for NO_2, $PM_{2.5}$, and O_3 for the most, medium, and least disadvantaged communities. Day-to-day exposure fluctuations decreased for NO_2 (Fig. 5A) and O_3 (Fig. 5C) for all communities, indicating more stable air quality over time. The reduction in exposure variations led to a decrease in the disparity of exposure fluctuations for NO_2 (slopes of −0.081 and −0.048 with $P < 0.001$ for disadvantaged versus advantaged). The reduction in exposure fluctuations remained similar for all communities for O_3 (slopes of −0.043 and −0.044 with $P = 0.85$ for disadvantaged versus advantaged). This implies that all communities maintained stable air quality despite vulnerable communities still having the highest air pollution exposure variations. The day-to-day exposure fluctuations of $PM_{2.5}$ (Fig. 5B) increased across all communities indicate a greater

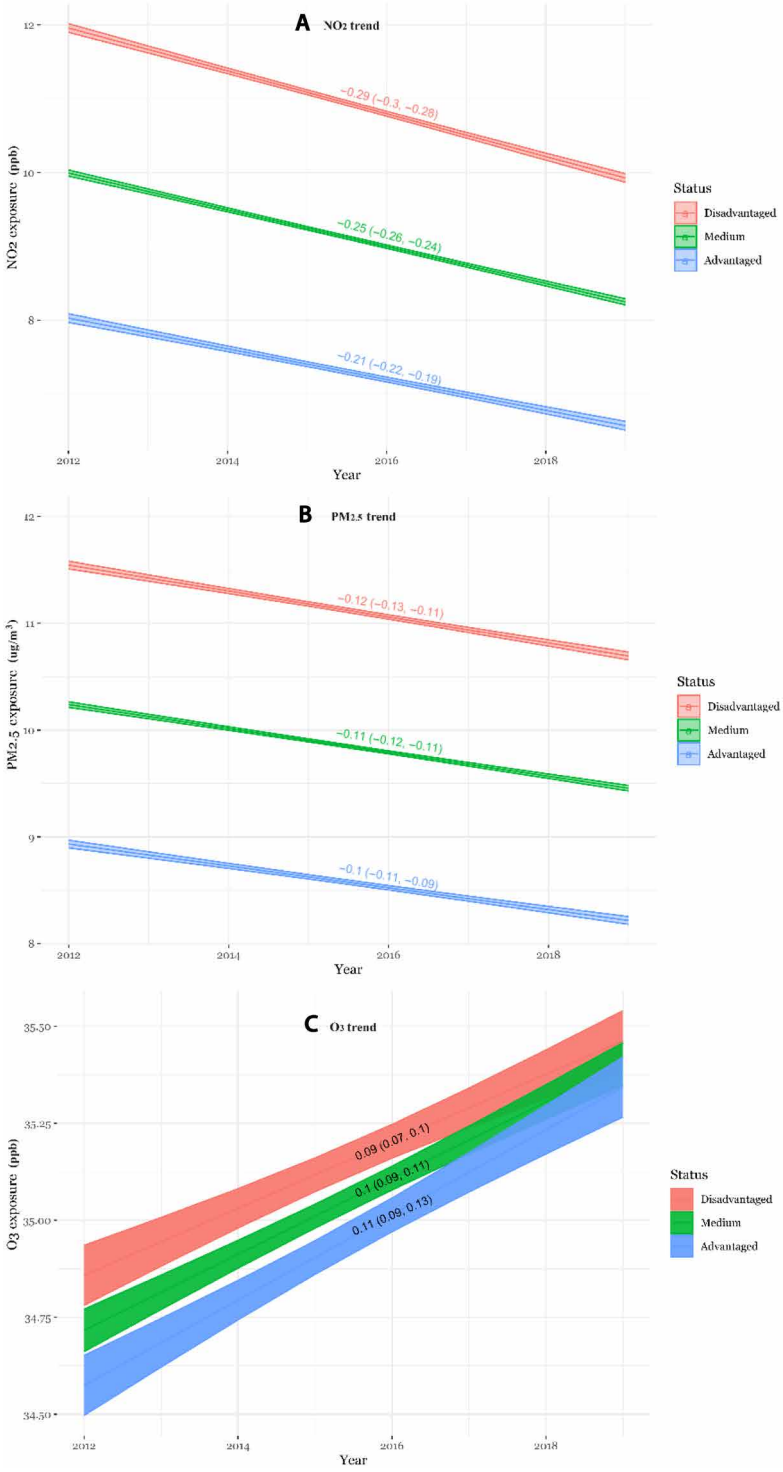

Fig. 4. Mean annual air pollution concentration trends for most disadvantaged (red), least disadvantaged (blue), and moderate disadvantaged (green) communities from 2012 to 2019. The trends illustrate variations in mean annual air pollutant concentrations of (**A**) nitrogen dioxide (NO_2), (**B**) fine particulate matter ($PM_{2.5}$), and (**C**) ozone (O_3) across different levels of community disadvantage. Numbers presented on the figures are slopes and associated 95% confidence intervals.

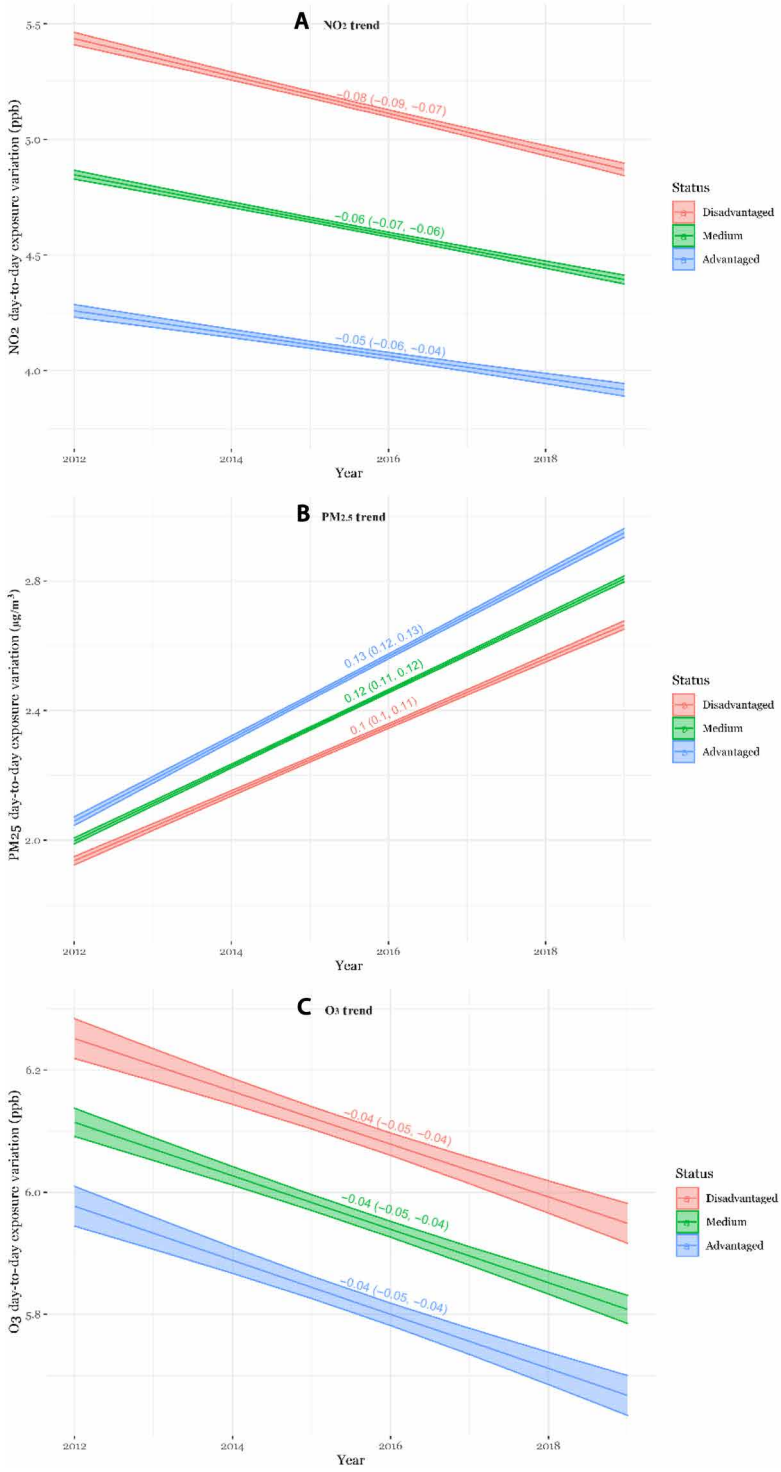

Fig. 5. Day-to-day exposure fluctuations for most disadvantaged (red), least disadvantaged (blue), and moderate disadvantaged (green) communities from 2012 to 2019. The graph illustrates the variations in daily exposures within a year for the air pollutants (**A**) nitrogen dioxide (NO_2), (**B**) fine particulate matter ($PM_{2.5}$) and (**C**) ozone (O_3) over the eight year time period across different levels of community disadvantage.

volatility in air quality conditions; we attributed this to the increased frequency and intensity of wildfires experienced from 2012 to 2019 (*30*).

To confirm the increasing daily variations of $PM_{2.5}$ concentrations despite an overall decrease in $PM_{2.5}$ from 2012 to 2019, we conducted a comprehensive analysis and detailed it in the Supplementary Materials. The analysis, focusing on wildfire occurrences in California throughout 2018, highlights a significant relationship between wildfire events and ambient $PM_{2.5}$ concentrations. The observed effects demonstrate statistical significance across various analyses, indicating a substantial impact of wildfires on heightened $PM_{2.5}$ concentrations. These findings support our assertion of increased day-to-day fluctuations in air quality attributed to wildfires.

DISCUSSION

Regulatory actions and technology advances over the past decade have led to a decrease in air pollutant concentrations (*31*–*33*). The improved environmental conditions have provided opportunities for enhancing air pollution modeling and identifying exposure disparities. In this study, we used extensive datasets spanning 2012 to 2019, including three air pollution monitoring sources and multiple other data sources, including traffic data, remotely sensed pollutants, weather information, vegetation indices, land use and land cover data, and different geographic features. These datasets enabled us to generate precise and detailed air pollution surfaces for California, surpassing any previous estimates. These surfaces were used to identify California's air pollution exposure disparities at the community level (census tract) based on geography, race-ethnicity, socioeconomic disadvantage, and temporal trends.

Focus on identification of small-area variations of pollutant concentrations

Our primary focus in LUR modeling was to identify small-area variations in pollutant concentrations at a fine spatial scale. It is important to highlight that our study context differs from other studies, such as that of Di *et al.* (*34*). While Di *et al.* analyzed a large dataset covering the entire U.S. with a resolution of 1 km from 1928 monitoring stations, our study concentrated specifically on California, using 850 air quality monitoring stations for $PM_{2.5}$. This difference in spatial resolution has significant implications for the ability to discern exposure disparities between disadvantaged and advantaged communities, a critical aspect of our research. Our adjusted R^2 value of 65% reflects a substantial overall correlation of more than 80% between our predictors and pollutant concentrations, underscoring the robustness of our modeling framework. While different modeling approaches may yield higher R^2 values, our focus remains on delivering insights into small-scale variations in air quality, rather than using dummy variables for climate regions to enhance model prediction power, aligning with the goals of our study.

Air pollution exposure disparities

Our findings revealed consistently higher mean annual concentrations of NO_2 and $PM_{2.5}$ in disadvantaged communities compared to advantaged communities. Our O_3 results tell a somewhat different story. While we observed that advantaged communities exhibited higher O_3 concentrations in most metropolitan areas than disadvantaged communities, statewide statistics showed that 24.14% of disadvantaged communities and 19.92% of advantaged communities experienced high O_3 concentrations. This pattern can be attributed to NO_X titration, where ozone concentrations tend to be lower within cities because of the reaction between ozone and NO_X, leading to relatively higher ozone levels at the city margins. This phenomenon explains why the exposure patterns for ozone differ from those of NO_2 and $PM_{2.5}$. These results are consistent with previous research (*35*, *36*), albeit our community-level analysis offers a more refined understanding compared to studies based on coarser geographic scales, such as zip codes. Furthermore, we found that communities with a higher proportion of minority populations were exposed to elevated concentrations of NO_2 and $PM_{2.5}$ compared to predominantly white communities, which aligns with existing literature (*6*, *37*, *38*). Our study revealed that disadvantaged communities are consistently exposed to higher air pollution concentrations than advantaged communities. Disadvantaged communities are often located near industrial facilities and manufacturing plants (*3*–*5*), major roadways (*6*–*8*), and other sources of pollution, leading to higher concentrations in nearby areas. They may have fewer parks and green spaces to help trap pollutants in the area and lead to higher exposure levels for residents (*39*, *40*). The high levels of air pollution exposure have serious health consequences, including increased risk of respiratory (*41*, *42*) and cardiovascular diseases (*43*–*45*) and even premature death (*46*, *47*). Poor health due to air pollution can lead to increased health care costs (*48*, *49*) and reduced workforce productivity (*49*, *50*) in disadvantaged communities.

For day-to-day fluctuations, the reduction in exposure variations led to a decrease in the disparity of exposure fluctuations for NO_2, indicating that vulnerable communities experienced more consistent air quality despite still having the highest air pollution exposure and variations. The day-to-day exposure fluctuations of $PM_{2.5}$ increase across all communities is correlated with the increased frequency and intensity of wildfires experienced in recent years. The advantaged communities exhibited both elevated $PM_{2.5}$ exposure variations and experienced a further surge in day-to-day fluctuations during the 2012–2019 period, very likely because of their predominant residence in suburban and rural regions, where the impacts of wildfires were most pronounced.

The research reveals a decrease in overall pollution concentrations, yet persistent disparities in exposure remain prevalent in disadvantaged communities. Urgent efforts, including regulatory measures, are essential to minimize pollution discrepancies in marginalized areas and ensure equitable exposure to clean air. The regulatory policies and interventions should be implemented at all levels of government, including local, regional, and national, aimed at addressing air pollution disparities. While exposure disparities often result from systemic injustices, regulatory measures can play a crucial role in mitigating these discrepancies by enforcing pollution controls, implementing stricter emission standards, and promoting environmental justice initiatives. These measures may include but are not limited to zoning regulations, emission regulations for industrial facilities, vehicle emission standards, and environmental justice policies aimed at protecting vulnerable communities.

The study highlights the correlation between increased frequency and intensity of wildfires and heightened day-to-day exposure variations in specific regions. Although we only used 1 year of data to conduct our analysis, our hypothesis of this trend for recent years is supported by literature. Recent years have seen a marked increase in the frequency and intensity of wildfires in California, driven by a combination of climate change, extended dry seasons, and increased

fuel loads. Wildfire frequency refers to the number of distinct wildfire events, at least 100 acres in timber or 300 acres in grasslands to be counted, per year or per fire season within a given geographic region. Intensity, in this context, refers to the severity and destructiveness of wildfires, often measured by the acreage burned and the energy released during the fires. The California Department of Forestry and Fire Protection (Cal Fire) has documented this trend, noting that the 2020 wildfire season was one of the most severe on record, with nearly 4.3 million acres burned and five of the six largest fires in California's history occurring that year (*51*). Williams *et al.* (*52*) examined the direct impacts of human-induced climate change on wildfire behavior, providing evidence of increased fire frequency and intensity. Similarly, Goss *et al.* (*53*) discussed how climate change has amplified extreme autumn wildfire conditions, making such events more frequent and severe. Keeley and Syphard (*54*) reviewed historical wildfire ignition sources, demonstrating an upward trend in wildfire occurrences. Westerling's (*55*) projections for California's Fourth Climate Change Assessment further support these findings, indicating substantial increases in wildfire frequency and intensity under warming climate scenarios. The comprehensive annual reports from Cal Fire (*56*) underscore the increasing acreage burned and the growing severity of wildfires in recent seasons, reinforcing the critical impact of these environmental changes on California's wildfire dynamics. Proactive strategies are needed to mitigate the impact of natural disasters on air quality, emphasizing the importance of comprehensive approaches to safeguard communities from environmental challenges. To accurately identify the day-to-day impacts of wildfires, we recommend a temporal resolution of daily or sub-daily data and a spatial resolution finer than 1 km. Resolutions coarser than 5 km would significantly dilute the wildfire impact due to the smoothing effect within such large pixels.

It is confirmed not only by this research but also by other studies (*57*–*59*) that the unequal distribution of air pollution exacerbates health disparities, perpetuating environmental injustice. The disadvantaged communities, being in close proximity to air pollution emissions sources, have likely experienced notable improvements in air quality, thus benefiting most from the regulatory efforts aimed at reducing air pollution (*60*). These improvements underscore the progress made toward environmental justice due to these regulatory actions. However, environmental injustice will persist until comprehensive policies are fully implemented at both local and national levels to address systemic disparities in exposure to air pollution.

Limitations

Despite generating terabytes of high spatiotemporal resolution data for our exposure assessment (30 m for modeling and 100 m for surface generation), we did not account for diurnal variations due to the substantial computational power and storage space required. This limitation could be addressed when computer clusters with extensive storage space become more widely accessible.

The study used data from 2012 to 2019. Therefore, the observed trends may not fully capture recent changes or emerging patterns in air pollution exposure disparities, such as the impact of COVID-19 on traffic, industrial operations, and other activities that could have influenced concentrations in more recent years. The findings should be interpreted within the context of the studied time frame.

In defining advantaged and disadvantaged communities, we relied on CalEnviroScreen cumulative scores. CalEnviroScreen assigns equal weights to all environmental factors when determining the final cumulative score, which may have misclassified some communities as disadvantaged. Translating these findings into actionable policies or interventions to address environmental exposure disparities in disadvantaged communities requires careful consideration of additional factors, including socioeconomic factors, community-specific characteristics, and stakeholder engagement.

While our LUR modeling approach offers valuable insights into small-area variations in pollutant concentrations, it is essential to acknowledge certain limitations. The relatively low adjusted R^2 value for $PM_{2.5}$, particularly when compared to other models like Di *et al.* (*34*), prompts consideration of these limitations. One primary constraint lies in the spatial resolution of our dataset, which, focused solely on California, may not capture the broader variability present across the entire U.S. In addition, our selection of predictors, while historically significant and directionally associated with measured concentrations, may not encompass all relevant factors influencing $PM_{2.5}$ concentrations. Furthermore, the inability of our LUR models to effectively handle hundreds of predictors with potential collinearity may contribute to the observed R^2 values. We have been limiting our final number of predictors to less than 20 in our historical LUR modeling. Despite these limitations, our modeling framework remains robust, offering substantial insights into pollutant concentration variations at small-area variations.

Outlook

Regulations and technological improvements such as vehicle emissions control, stricter standards for refineries and factories, and increased use of clean power generation have contributed to a steady decline in criteria air pollutants in California (*61*), as confirmed by this research. Concentrations of NO_2 and $PM_{2.5}$ were estimated to have decreased from 2012 to 2019 across all communities, with the most notable reductions observed in the disadvantaged communities. However, O_3 concentrations increased in all communities during the same period, with the largest increase observed in advantaged communities. This finding aligns with the understanding that NO_2 and $PM_{2.5}$ are negatively associated with O_3 concentrations due to photochemical reactions (*62*–*64*).

Environmental justice advocates and policymakers argue that disadvantaged communities face a disproportionate burden from environmental hazards (*65*). However, quantitative assessments of environmental justice, particularly comprehensive comparisons between communities, are still relatively rare in the literature (*66*, *67*). Most existing air pollution models and surfaces have limited spatial resolution, which hinders effective differentiation of air pollution exposure between disadvantaged and advantaged communities. By using high spatiotemporal resolution models and surfaces developed in this study, we were able to compare air pollution exposure disparities between disadvantaged and advantaged communities by overlaying air pollution surfaces with CalEnviroScreen disadvantage status. In addition, we identified regions of highest air pollution concerns throughout California, as well as local concerns within metropolitan regions. We further identified disparities in air pollution exposure based on race-ethnicity and examined the temporal trends (overall exposure and day-to-day fluctuations) in air pollution exposure for disadvantaged and advantaged communities. The study contributes valuable insights into air pollution exposure disparities and underscores the importance of integrating multiple data sources and advanced modeling techniques to enhance our understanding of the complex relationship between air pollution, health,

and disparities. These findings provide policymakers with an effective tool to identify and implement interventions to reduce air pollution exposure disparities in disadvantaged communities.

MATERIALS AND METHODS

Our study used a comprehensive methodology to develop high-resolution air pollution models and surfaces for NO_2, $PM_{2.5}$, and O_3 across California from 2012 to 2019. We integrated diverse data sources and used various scripting languages to process and analyze extensive datasets.

We processed daily traffic data from California highways and parcel-level land use data from 58 counties using R scripting, which enabled the derivation of daily traffic surfaces and incorporation of detailed land use information into our modeling approach. In addition, Google Earth Engine (JavaScript) was used to process land cover data, vegetation indices, impervious surfaces, meteorological conditions, and aerosol optical depth data, providing critical spatial predictors at high resolution.

Our study integrated daily air quality measurements from regulatory monitoring stations, fixed-site saturation monitoring in specific counties, and Google Streetcar mobile monitoring across different regions into a unified modeling framework. This diverse dataset facilitated the development of daily LUR models using the D/S/A machine learning algorithm (*68*, *69*). During the modeling process, we aimed for fine spatial resolution (30 m) while managing multicollinearity and limiting predictor complexity for enhanced interpretability.

Spatial and temporal disparities in air pollution exposure were analyzed at the community level, defining disadvantaged and advantaged communities based on CalEnviroScreen scores (*29*). *T* tests were conducted to compare air pollution exposure between these community types. Linear models were used to explore connections between demographic factors and air pollution levels, focusing separately on NO_2, $PM_{2.5}$, and O_3. Furthermore, we investigated the impact of wildfire events on $PM_{2.5}$ concentrations during 2018, using wildfire occurrence data from Cal Fire and using statistical techniques to assess the relationship between wildfire events and ambient $PM_{2.5}$ concentrations using regulatory air quality monitors across California.

For more detailed information on our methodologies and analyses, please refer to the Supplementary Materials accompanying this manuscript. This supplementary content provides additional insights into our study approach.

Supplementary Materials

This PDF file includes:

Supplementary Text
Figs. S1 to S4
Tables S1 to S5

REFERENCES AND NOTES

1. J. Liu, M. Bechle, L. P. Clark, S.-Y. Kim, J. Marshall, Environmental Justice for Criteria Air Pollutants in the United States during 1990, 2000, and 2010, ISES-ISEE 2018 Joint Annual Meeting: Addressing Complex Local and Global Issues in Environmental Exposure and Health (*ISEE Conference Abstracts 2018*), 24 September 2018.
2. A. Hajat, C. Hsia, M. S. O'Neill, Socioeconomic disparities and air pollution exposure: A global review. *Curr. Environ. Health Rep.* **2**, 440–450 (2015).
3. S. A. Perlin, R. W. Setzer, J. Creason, K. Sexton, Distribution of industrial air emissions by income and race in the United States: An approach using the toxic release inventory. *Environ. Sci. Technol.* **29**, 69–80 (1995).
4. G. Walker, G. Mitchell, J. Fairburn, G. Smith, Industrial pollution and social deprivation: Evidence and complexity in evaluating and responding to environmental inequality. *Local Environ.* **10**, 361–377 (2005).
5. S. A. Perlin, D. Wong, K. Sexton, Residential proximity to industrial sources of air pollution: Interrelationships among race, poverty, and age. *J. Air Waste Manage. Assoc.* **51**, 406–421 (2001).
6. D. Houston, J. Wu, P. Ong, A. Winer, Structural disparities of urban traffic in Southern California: Implications for vehicle-related air pollution exposure in minority and high-poverty neighborhoods. *J. Urban Aff.* **26**, 565–592 (2004).
7. D. Houston, W. Li, J. Wu, Disparities in exposure to automobile and truck traffic and vehicle emissions near the Los Angeles–Long Beach port complex. *Am. J. Public Health* **104**, 156–164 (2014).
8. T. K. Boehmer, S. L. Foster, J. R. Henry, E. L. Woghiren-Akinnifesi, F. Y. Yip, Centers for Disease Control and Prevention (CDC), Residential proximity to major highways—United States, 2010. *MMWR Suppl.* **62**, 46–50 (2013).
9. L. Patel, E. Friedman, S. A. Johannes, S. S. Lee, H. G. O'Brien, S. E. Schear, Air pollution as a social and structural determinant of health. *J. Clim. Change Health* **3**, 100035 (2021).
10. L. G. Hooper, J. D. Kaufman, Ambient air pollution and clinical implications for susceptible populations. *Ann. Am. Thorac. Soc.* **15**, S64–S68 (2018).
11. American Lung Association, Urban air pollution and health inequities: A workshop report. *Environ. Health Perspect.* **109**, 357–374 (2001).
12. X. Xie, I. Semanjski, S. Gautama, E. Tsiligianni, N. Deligiannis, R. T. Rajan, F. Pasveer, W. Philips, A review of urban air pollution monitoring and exposure assessment methods. *ISPRS Int. J. Geo Inf.* **6**, 389 (2017).
13. L. de Preux, D. Rizmie, D. Fecht, J. Gulliver, W. Wang, Does it measure up? A comparison of pollution exposure assessment techniques applied across hospitals in England. *Int. J. Environ. Res. Public Health* **20**, 3852 (2023).
14. P. H. Ryan, G. K. LeMasters, A review of land-use regression models for characterizing intraurban air pollution exposure. *Inhal. Toxicol.* **19**, 127–133 (2007).
15. G. Hoek, R. Beelen, K. de Hoogh, D. Vienneau, J. Gulliver, P. Fischer, D. Briggs, A review of land-use regression models to assess spatial variation of outdoor air pollution. *Atmos. Environ.* **42**, 7561–7578 (2008).
16. J. G. Su, P. K. Hopke, Y. L. Tian, N. Baldwin, S. W. Thurston, K. Evans, D. Q. Rich, Modeling particulate matter concentrations measured through mobile monitoring in a deletion/substitution/addition approach. *Atmos. Environ.* **122**, 477–483 (2015).
17. X. Hu, J. H. Belle, X. Meng, A. Wildani, L. A. Waller, M. J. Strickland, Y. Liu, Estimating $PM_{2.5}$ concentrations in the conterminous United States using the random forest approach. *Environ. Sci. Technol.* **51**, 6936–6944 (2017).
18. Y. Zhan, Y. Luo, X. Deng, K. Zhang, M. Zhang, M. L. Grieneisen, B. Di, Satellite-based estimates of daily NO_2 exposure in China using hybrid random forest and spatiotemporal kriging model. *Environ. Sci. Technol.* **52**, 4180–4189 (2018).
19. C. Brokamp, R. Jandarov, M. Hossain, P. Ryan, Predicting daily urban fine particulate matter concentrations using a random forest model. *Environ. Sci. Technol.* **52**, 4173–4179 (2018).
20. G. Chen, S. Li, L. D. Knibbs, N. Hamm, W. Cao, T. Li, J. Guo, H. Ren, M. J. Abramson, Y. Guo, A machine learning method to estimate $PM_{2.5}$ concentrations across China with remote sensing, meteorological and land use information. *Sci. Total Environ.* **636**, 52–60 (2018).
21. X. Zhang, Y. Chu, Y. Wang, K. Zhang, Predicting daily $PM_{2.5}$ concentrations in Texas using high-resolution satellite aerosol optical depth. *Sci. Total Environ.* **631**, 904–911 (2018).
22. S. V. Deo, Y. Elgudin, I. Motairek, F. Ho, R. D. Brook, J. Su, S. Fremes, P. deSouza, O. Hahad, S. Rajagopalan, Air pollution and adverse cardiovascular events after coronary artery bypass grafting: A 10-year nationwide study. *JACC: Adv.* **3**, 100781 (2024).
23. K. Osharkey, S. Mitra, S. A. Paik, J. Su, T. Chow, B. Ritz, Multipollutant Associations Between Air Pollution and Autism Spectrum Disorder in California: How Sociodemographics and Region Impact Risk, in *ISEE Conference Abstracts, 35th Annual Conference of the International Society of Environmental Epidemiology* (ISEE 2023), pp. EP-088; https://doi.org/10.1289/isee.2023.EP-088.
24. Y.-Y. Meng, Y. Yu, S. H. Babey, J. Su, Long-term air pollution exposures on type 2 diabetes prevalence and medication use. *Hygiene Environ. Health Adv.* **7**, 100062 (2023).
25. Y. Yu, J. Su, M. Jerrett, K. C. Paul, E. Lee, I.-F. Shih, M. Haan, B. Ritz, Air pollution and traffic noise interact to affect cognitive health in older Mexican Americans. *Environ. Int.* **173**, 107810 (2023).
26. J. G. Su, M. A. Barrett, V. Combs, K. Henderson, D. Van Sickle, C. Hogg, G. Simrall, S. S. Moyer, P. Tarini, O. Wojcik, Identifying impacts of air pollution on subacute asthma symptoms using digital medication sensors. *Int. J. Epidemiol.* **51**, 213–224 (2022).
27. Y. Yu, M. Jerrett, K. C. Paul, J. Su, I.-F. Shih, J. Wu, E. Lee, K. Inoue, M. Haan, B. Ritz, Ozone exposure, outdoor physical activity, and incident type 2 diabetes in the SALSA cohort of older Mexican Americans. *Environ. Health Perspect.* **129**, 097004 (2021).

28. A. M. Williams, D. J. Phaneuf, M. A. Barrett, J. G. Su, Short-term impact of PM2. 5 on contemporaneous asthma medication use: Behavior and the value of pollution reductions. *Proc. Natl. Acad. Sci. U.S.A.* **116**, 5246–5253 (2019).
29. L. Zeise, J. Blumenfeld, L. August, B. Komal, L. Plummer, K. Ranjbar, A. Slocombe, W. Wieland, CalEnviroScreen 4.0. California Office of Environmental Health Hazard Assessment (OEHHA) (2021); https://oehha.ca.gov/calenviroscreen.
30. M. R. Rossiello, A. Szema, Health effects of climate change-induced wildfires and heatwaves. *Cureus* **11**, e4771 (2019).
31. A. W. Correia, C. A. Pope III, D. W. Dockery, Y. Wang, M. Ezzati, F. Dominici, Effect of air pollution control on life expectancy in the United States. *Epidemiology* **24**, 23–31 (2013).
32. K. Kuklinska, L. Wolska, J. Namiesnik, Air quality policy in the U.S. and the EU–A review. *Atmos. Pollut. Res.* **6**, 129–137 (2015).
33. S. K. Thakrar, S. Balasubramanian, P. J. Adams, I. M. Azevedo, N. Z. Muller, S. N. Pandis, S. Polasky, C. A. Pope III, A. L. Robinson, J. S. Apte, Reducing mortality from air pollution in the United States by targeting specific emission sources. *Environ. Sci. Technol. Lett.* **7**, 639–645 (2020).
34. Q. Di, L. Dai, Y. Wang, A. Zanobetti, C. Choirat, J. D. Schwartz, F. Dominici, Association of short-term exposure to air pollution with mortality in older adults. *JAMA* **318**, 2446–2456 (2017).
35. H. Rickenbacker, F. Brown, M. Bilec, Creating environmental consciousness in underserved communities: Implementation and outcomes of community-based environmental justice and air pollution research. *Sustain. Cities Soc.* **47**, 101473 (2019).
36. C. M. Anderson, K. A. Kissel, C. B. Field, K. J. Mach, Climate change mitigation, air pollution, and environmental justice in California. *Environ. Sci. Technol.* **52**, 10829–10838 (2018).
37. K. Sexton, H. Gong Jr., J. C. Bailar, J. G. Ford, D. R. Gold, W. E. Lambert, M. J. Utell, Air pollution health risks: Do class and race matter? *Toxicol. Ind. Health* **9**, 843–878 (1993).
38. J. G. Su, M. Jerrett, A. de Nazelle, J. Wolch, Does exposure to air pollution in urban parks have socioeconomic, racial or ethnic gradients? *Environ. Res.* **111**, 319–328 (2011).
39. P. Dadvand, I. Rivas, X. Basagaña, M. Alvarez-Pedrerol, J. Su, M. D. C. Pascual, F. Amato, M. Jerret, X. Querol, J. Sunyer, The association between greenness and traffic-related air pollution at schools. *Sci. Total Environ.* **523**, 59–63 (2015).
40. I. Jarvis, Z. Davis, H. Sbihi, M. Brauer, A. Czekajlo, H. W. Davies, S. E. Gergel, M. Guhn, M. Jerrett, M. Koehoorn, Assessing the association between lifetime exposure to greenspace and early childhood development and the mediation effects of air pollution and noise in Canada: A population-based birth cohort study. *Lancet Planet. Health* **5**, e709–e717 (2021).
41. J. G. Su, M. A. Barrett, K. Henderson, O. Humblet, T. Smith, J. W. Sublett, L. Nesbitt, C. Hogg, D. Van Sickle, J. L. Sublett, Feasibility of deploying inhaler sensors to identify the impacts of environmental triggers and built environment factors on asthma short-acting bronchodilator use. *Environ. Health Perspect.* **125**, 254–261 (2017).
42. D. Kim, Z. Chen, L.-F. Zhou, S.-X. Huang, Air pollutants and early origins of respiratory diseases. *Chronic Dis. Transl. Med.* **4**, 75–94 (2018).
43. F. Dominici, R. D. Peng, M. L. Bell, L. Pham, A. McDermott, S. L. Zeger, J. M. Samet, Fine particulate air pollution and hospital admission for cardiovascular and respiratory diseases. *JAMA* **295**, 1127–1134 (2006).
44. B.-J. Lee, B. Kim, K. Lee, Air pollution exposure and cardiovascular disease. *Toxicol Res.* **30**, 71–75 (2014).
45. B. A. Franklin, R. Brook, C. A. Pope III, Air pollution and cardiovascular disease. *Curr. Probl. Cardiol.* **40**, 207–238 (2015).
46. J. Lelieveld, J. S. Evans, M. Fnais, D. Giannadaki, A. Pozzer, The contribution of outdoor air pollution sources to premature mortality on a global scale. *Nature* **525**, 367–371 (2015).
47. S. Khomenko, M. Cirach, E. Pereira-Barboza, N. Mueller, J. Barrera-Gómez, D. Rojas-Rueda, K. de Hoogh, G. Hoek, M. Nieuwenhuijsen, Premature mortality due to air pollution in European cities: A health impact assessment. *Lancet Planet. Health* **5**, e121–e134 (2021).
48. A. Baciu, Y. Negussie, A. Geller, J. N. Weinstein, National Academies of Sciences, Engineering, and Medicine, "The Need to Promote Health Equity," in *Communities in action: Pathways to health equity* (National Academies Press, 2017).
49. L. D. Frank, N. Iroz-Elardo, K. E. MacLeod, A. Hong, Pathways from built environment to health: A conceptual framework linking behavior and exposure-based impacts. *J. Transp. Health* **12**, 319–335 (2019).
50. M. C. Arcaya, A. L. Arcaya, S. V. Subramanian, Inequalities in health: Definitions, concepts, and theories. *Glob. Health Action* **8**, 27106 (2015).
51. Cal Fire, "2020 Fire Season Incident Archive" (2020). [Accessed on 25 June 2024]; https://fire.ca.gov/incidents/2020.
52. A. P. Williams, J. T. Abatzoglou, A. Gershunov, J. Guzman-Morales, D. A. Bishop, J. K. Balch, D. P. Lettenmaier, Observed impacts of anthropogenic climate change on wildfire in California. *Earth's Future* **7**, 892–910 (2019).
53. M. Goss, D. L. Swain, J. T. Abatzoglou, A. Sarhadi, C. A. Kolden, A. P. Williams, N. S. Diffenbaugh, Climate change is increasing the likelihood of extreme autumn wildfire conditions across California. *Environ. Res. Lett.* **15**, 094016 (2020).
54. J. E. Keeley, A. D. Syphard, Historical patterns of wildfire ignition sources in California ecosystems. *Int. J. Wildland Fire* **27**, 781–799 (2018).
55. A. L. Westerling, *Wildfire Simulations for California's Fourth Climate Change Assessment: Projecting Changes in Extreme Wildfire Events with a Warming Climate: A Report for California's Fourth Climate Change Assessment* (California Energy Commission Sacramento, CA, 2018).
56. Cal Fire, "2023 Fire Season Incident Archive." (2023). [Accessed on 25 June 2024]; https://fire.ca.gov/incidents/2023/.
57. J. Pearce, S. Kingham, Environmental inequalities in New Zealand: A national study of air pollution and environmental justice. *Geoforum* **39**, 980–993 (2008).
58. T. G. Leech, E. A. Adams, T. D. Weathers, L. K. Staten, G. M. Filippelli, Inequitable chronic lead exposure: A dual legacy of social and environmental injustice. *Fam. Community Health* **39**, 151–159 (2016).
59. G. S. Smith, E. Anjum, C. Francis, L. Deanes, C. Acey, Climate change, environmental disasters, and health inequities: The underlying role of structural inequalities. *Curr. Environ. Health Rep.* **9**, 80–89 (2022).
60. J. G. Su, Y.-Y. Meng, M. Pickett, E. Seto, B. Ritz, M. Jerrett, Identification of effects of regulatory actions on air quality in goods movement corridors in California. *Environ. Sci. Technol.* **50**, 8687–8696 (2016).
61. J. G. Su, Y.-Y. Meng, X. Chen, J. Molitor, D. Yue, M. Jerrett, Predicting differential improvements in annual pollutant concentrations and exposures for regulatory policy assessment. *Environ. Int.* **143**, 105942 (2020).
62. M. A. Zoran, R. S. Savastru, D. M. Savastru, M. N. Tautan, Assessing the relationship between ground levels of ozone (O_3) and nitrogen dioxide (NO_2) with coronavirus (COVID-19) in Milan, Italy. *Sci. Total Environ.* **740**, 140005 (2020).
63. M. M. Shareef, T. Husain, B. Alharbi, Analysis of relationship between O_3, NO, and NO_2 in Riyadh, Saudi Arabia. *Asian. J. Atmos. Environ.* **12**, 17–29 (2018).
64. J. Ngarambe, S. J. Joen, C.-H. Han, G. Y. Yun, Exploring the relationship between particulate matter, CO, SO_2, NO_2, O_3 and urban heat island in Seoul, Korea. *J. Hazard. Mater.* **403**, 123615 (2021).
65. J. G. Su, R. Morello-Frosch, B. M. Jesdale, A. D. Kyle, B. Shamasunder, M. Jerrett, An Index for Assessing Demographic Inequalities in Cumulative Environmental Hazards with Application to Los Angeles, California. *Environ. Sci. Technol.* **43**, 7626–7634 (2009).
66. J. Faust, L. August, A. Slocombe, S. Prasad, W. Wieland, V. Cogliano, C. M. Cummings, California's environmental justice mapping tool: Lessons and insights from calenviroscreen. *Envtl. L. Rep.* **51**, 10684 (2021).
67. L. August, K. Bangia, J. Faust, A. Slocombe, W. Wieland, A mapping tool to identify environmental justice communities in California. How it is used and what type of communities are identified. American Public Health Association (APHA)'s 2018 Annual Meeting & Expo, 10 to 14 November 2018.
68. B. S. Beckerman, M. Jerrett, M. Serre, R. V. Martin, S.-J. Lee, A. van Donkelaar, Z. Ross, J. Su, R. T. Burnett, A hybrid approach to estimating national scale spatiotemporal variability of $PM_{2.5}$ in the contiguous United States. *Environ. Sci. Technol.* **47**, 7233–7241 (2013).
69. J. G. Su, M. Jerrett, Y. Y. Meng, M. Pickett, B. Ritz, Integrating smart-phone based momentary location tracking with fixed site air quality monitoring for personal exposure assessment. *Sci. Total Environ.* **506**, 518–526 (2015).

Acknowledgments

Funding: This work was funded by the California Air Resources Board grant 19RD004 (J.G.S., contact; M.B., co-PI). **Author contributions:** Conceptualization: J.G.S., M.B., and M.J. Data curation: J.G.S. and V.V. Formal analysis: J.G.S., V.V., and S.A. Funding acquisition: J.G.S. and M.B. Investigation: J.G.S., M.B., V.V., and E.Sh. Methodology: J.G.S., M.J., M.B., and V.V. Project administration: J.G.S. and M.B. Resources: J.G.S. and V.V. Software: J.G.S., V.V., and S.A. Supervision: J.G.S., M.B., J.B., and M.J. Validation: J.G.S., M.B., V.V., and S.A. Visualization: J.G.S., V.V., M.B., and S.A. Writing—original draft: J.G.S., M.B., S.A., V.V., and R.H. Writing—review and editing: J.G.S., M.B., S.A., V.V., E.Sa., E. Sh., E.Y., R.H., and J.B. **Competing interests:** M.B. and V.V. are Propeller Health and ResMed employees and receive salary and stock. The other authors declare that they have no actual or potential competing interests. **Data and materials availability:** All the R scripts for LUR modeling, JavaScript for Google Earth Engine data processing, and Python scripts for surface generation will be available through Dryad data repository, 10.5061/dryad.6djh9w18p. Additionally, the daily air pollutant surfaces of 100-m resolution for NO_2, $PM_{2.5}$, and O_3 for years 2012 to 2019 for the state of California are available on Dryad with the same DOI. All other data needed to evaluate the conclusions of the paper are present in the paper and/or the Supplementary Materials.

Submitted 16 November 2023
Accepted 8 July 2024
Published 7 August 2024
10.1126/sciadv.adm9986